Journal of Catalysis **192,** 98–107 (2000)
doi:10.1006/jcat.2000.2824, available online at http://www.idealibrary.com on IDEAL®

Periodic Trends in Hydrotreating Catalysis: Thiophene Hydrodesulfurization over Carbon-Supported 4*d* Transition Metal Sulfides

E. J. M. Hensen, H. J. A. Brans, G. M. H. J. Lardinois, V. H. J. de Beer, J. A. R. van Veen, and R. A. van Santen

Schuit Institute of Catalysis, Eindhoven University of Technology, P.O. Box 513, 5600 MB Eindhoven, The Netherlands

Received September 14, 1999; revised January 13, 2000; accepted January 17, 2000

The kinetics of atmospheric gas-phase thiophene hydrodesulfurization (HDS) over five carbon-supported 4*d* transition metal sulfide catalysts (Mo, Ru, Rh, Pd, and CoMo) were studied. Reaction orders (thiophene, H_2S, and H_2), apparent activation energies, and pre-exponential factors were determined. The activity trends for these catalysts follow the well-known *volcano*-shape curve. The most active catalyst shows the lowest thiophene reaction order, which is taken to imply that a strong interaction between transition metal sulfide (TMS) and thiophene results in a high HDS activity. The kinetic results are interpreted in terms of trends in metal–sulfur bond energy. These trends are counter to commonly held correlations between metal–sulfur bond energy and periodic position of the transition metal. Both Sabatier's principle and the "bond energy model" appear to be inadequate in explaining the observed trends in kinetic parameters. Instead, an alternative proposal is made: the metal–sulfur bond strength at the TMS surface relevant to HDS catalysis depends on the sulfur coordination number of the surface metal atoms. Transition metals (TM) at the left-hand side of the periodic table, i.e., Mo, form stable sulfides, leading to a low sulfur addition energy under reaction conditions. The sulfur addition energy is the energy gained upon addition of a sulfur atom (e.g., in the form of thiophene) to the TMS. Over to the right-hand side of the periodic table, the stability of the TMS decreases due to lower bulk metal–sulfur bond energies. This can result in more coordinative unsaturation of the TM surface atoms and possibly the formation of incompletely sulfided phases with higher sulfur addition energies. At the right-hand side of the periodic table the activity decreases due to weak metal–sulfur interactions, leading to poisoning of the metallic state. © 2000 Academic Press

Key Words: **hydrotreating; thiophene; HDS; periodic trends; volcano curve; transition metal sulfides; metal–sulfur bond energy; H_2–D_2 equilibration.**

INTRODUCTION

In the oil refining industry the removal of heteroatoms (S, N, metals) from oil feedstock is one of the key operations for the production of clean transportation fuels. In addition to the necessity to process ever more heavy feeds and the concomitant higher HDS duty required, environmental awareness continuously leads to more stringent legislation with respect to the quality of these fuels. It seems questionable whether improvement of conventional catalytic systems, which include alumina-supported CoMo and NiMo mixed sulfide catalysts, can continue to meet these requirements. For a comprehensive outline of the current state of thinking with regard to these commercially important catalysts, the reader is referred to a series of reviews (1–5).

Alternatives to these mixed sulfides include the many transition metal sulfides (TMS) that have been found active in hydrotreating reactions. Pecoraro and Chianelli (6) systematically studied the activity of first, second, and third row bulk TMS in dibenzothiophene hydrodesulfurization at 30 bar hydrogen pressure in an autoclave. Most striking is the *volcano*-type plot found with activity maxima at the sulfides of Ru and Os for second row (4*d*) and third row (5*d*) TMS, respectively. Moreover, the activities of these TMSs may vary by 3 orders of magnitude across the periodic table. Similar trends were found for carbon-supported TMS in low-pressure thiophene HDS (7, 8), this time the maxima being at the sulfides of Rh and Ir.

The origin of these periodic trends is an issue of great debate. Pecoraro and Chianelli (6) explained the *volcano* plot in terms of Sabatier's principle: the stability of the surface complex formed by the organic sulfide must be intermediate to obtain high activity. Intermediate heats of formation lead to intermediate metal–sulfur bond strengths at the surface. Indeed, for second and third row TMS highest activity was found for those bulk TMSs having an intermediate heat of formation. Early quantum-chemical calculations gave more in-depth insight into the electronic nature of these TMSs (9–18). Nørskov, Clausen, and Topsøe (19) put forward a different concept: the differences in reaction rate for the various TMSs are dominated by the differences in the number of vacancies at the sulfide surface. Based on effective medium theory results, they concluded that the highest activity is found for the TMS with the lowest metal–sulfur bond energy. These results were supported by plotting the

0021-9517/00 $35.00
Copyright © 2000 by Academic Press
All rights of reproduction in any form reserved.

activity of the TMS as a function of the heat of formation per mole of metal–sulfur bond (20) rather than the heat of formation per mole of metal. The translation of these different explanations in terms of kinetic parameters for fundamental reaction steps in hydrotreating catalysis, e.g., for thiophene HDS, was outlined in a review by Hensen, De Beer, and Van Santen (21). The stage seems to be set to relate these different interpretations to kinetic experiments, which should allow us to obtain more detailed insight into the nature of these periodic trends.

In the present study a set of carbon-supported transition metals (Mo, Rh, Ru, and Pd) was used. The relative inertness of the carbon support enables the determination of intrinsic activities of the metal sulfides. For reasons of comparison, the results for CoMo/C are included. Atmospheric gas-phase thiophene HDS was used as a test reaction. Both the reaction orders of thiophene, H_2S, and H_2 and the apparent activation energies were determined. H_2–D_2 equilibration was used to study the activation of hydrogen on these TMS surfaces.

METHODS

Catalyst Preparation

Catalysts were prepared by pore volume impregnation of the carbon support with aqueous solutions of the corresponding metal salts (see Table 1) according to the procedure of Vissers *et al.* (22). carbon-supported Mo-containing catalysts (Mo/C; CoMo/C) were prepared by pore volume impregnation with ammoniacal solutions of $(NH_4)_6Mo_7O_{24}\cdot 4H_2O$ (Merck, >99.9%) and $Co(NO_3)_2\cdot 6H_2O$ (Merck, p.a.). For CoMo/C, nitrilo triacetic acid (NTA) was used as a complexing agent according to the procedure described by Van Veen *et al.* (23). The concentrations of the metal salt solutions for the monometallic catalysts were chosen so as to obtain a final metal (Me) loading of approximately 0.5 Me atoms per nm^2 of support surface area. A 125- to 250-μm sieve fraction of an activated carbon (Norit RX3-Extra) with a surface area of 1197 m^2/g and a pore volume of 1.0 ml/g was used as the carrier material.

TABLE 1

Metal Contents of Carbon-Supported Catalysts

Catalyst	Precursor metal salt	Supplier	Metal cont. (wt%)
Mo/C	$(NH_4)_6Mo_7O_{24}\cdot 4H_2O$	Merck, >99%	8.8
Ru/C	$RuCl_3\cdot H_2O$	Alfa	9.1
Rh/C	$RhCl_3\cdot 3H_2O$	Merck	9.2
Pd/C	$(NH_4)_2PdCl_4$	Alfa	9.5
CoMo/C	$(NH_4)_6Mo_7O_{24}\cdot 4H_2O$	Merck, >99%	6.0
	$Co(NO_3)_2\cdot 6H_2O$	Merck, >99%	1.1
	$N(C_3H_7O)_3$ (NTA)	Janssen Chimica, >97%	

Thiophene HDS

Kinetic measurements were carried out in an atmospheric quartz single-pass microflow reactor with an internal diameter of 4 mm. Gasified thiophene (Janssen Chimica, >99%) was obtained by passing hydrogen (Hoekloos, purity 99.95% additionally led through a gas-clean filter system to remove traces of oxygen, water, and hydrocarbons) through the liquid in a saturator that was kept at a constant temperature of 293 K. The required thiophene concentration was obtained by diluting this flow with pure hydrogen. Furthermore, additional flows of He (Hoekloos, purity 99.95% additionally led through a gas-clean filter system to remove traces of oxygen, water, and hydrocarbons) and a H_2S/H_2 mixture (Hoekloos, 10% H_2S) could be added to the reaction mixture. All gas flows were regulated by Brooks mass flow controllers that were driven by a computer system using DA converters. The reactor packing consisted of an amount of catalyst diluted with inert carbon of the same sieve fraction to achieve plug flow conditions. The amount of catalyst was chosen in such a way that during kinetic measurements the reactor was operated differentially, i.e., at conversions below 10%. The reaction product mixture was sampled every 20 min and analyzed by gas chromatography (UNICAM 610 Series equipped with a Chrompack CP-SIL 5 CB column).

Prior to reaction, catalysts were sulfided *in situ* in a H_2S/H_2 mixture (Hoekloos, 10% H_2S). The gas flow was kept at 60 Nml/min, while the catalyst was heated at a rate of 6 K/min upto 673 K. The temperature was then kept at 673 K for 2 h. After sulfidation, the catalyst was exposed to a mixture of 3.33×10^3 Pa thiophene and 1×10^3 Pa H_2S in hydrogen at a total gas flow rate of 100 Nml/min (standard conditions) at 673 K. After a stabilization period of 13 h, kinetic measurements were started.

All kinetic measurements were performed in the differential regime. This means that the reaction rate is proportional to the thiophene conversion. Reaction orders of thiophene (n_T), H_2S (n_S), and H_2 (n_H) were determined by measuring the reaction rate as a function of the partial pressure of the corresponding component (for thiophene, 1–6 kPa; for H_2S, 0.1–2 kPa; and for H_2, 25–97 kPa). The total gas flow was kept at 100 Nml/min. After each change in the conditions (composition of reaction mixture or temperature), the activity was measured for 3 h. The conversion was found to be constant during these intervals. The reaction order of a component was calculated by fitting the reaction rate to the partial pressure of this component using the power-rate law equation $R = k\cdot p^n$. The apparent activation energy was determined by evaluation of the reaction rate as a function of temperature. From this value and the reaction orders at a given temperature, the pre-exponential factor was calculated from

$$R = \upsilon_{\text{pre}}\, e^{-E_{\text{act}}^{\text{app}}/RT}\, p_T^{n_T} p_S^{n_S} p_H^{n_H}. \qquad [1]$$

H_2–D_2 Equilibration

A description of the recirculation apparatus and relevant procedures can be found elsewhere (24). Different pretreatment procedures were applied to the catalysts. In the standard experiment, the catalysts were sulfided according to the sulfidation procedure described previously and subsequently cooled to 423 K in flowing Ar. H_2–D_2 equilibration experiments both in the presence and in the absence of H_2S were carried out. In some experiments, the catalyst was cooled to 573 K in the sulfidation mixture subsequent to sulfidation. At this temperature, the catalyst was then exposed for 1 h to (i) 10% H_2S/H_2, (ii) 1% H_2S/H_2, or (iii) 0.1% H_2S/H_2 at a total gas flow rate of 100 Nml/min. After the catalyst was purged in flowing Ar (60 Nml/min) for 1 h, the H_2–D_2 equilibration activity was measured at 573 K.

RESULTS

Steady-State Thiophene HDS Activities

Steady-state thiophene HDS activities at 573 K and standard conditions for the different transition metal sulfides are shown in Fig. 1. It should be noted that the trend in steady-state activities between the various catalysts are equivalent to the trend in initial HDS activities at 673 K (25). The activity of Ag/C is so low at 573 K that this catalyst was not included in further kinetic experiments. The maximum in activity is found for Rh/C in line with previous studies by Vissers *et al.* (7) and Ledoux *et al.* (8). The activity differences between the different TMSs are lower than those reported in those references and are due to the higher H_2S partial pressure used in the present study. It is known that the sulfur tolerance of the sulfides of more noble metals is lower (26), a fact that will be corroborated by the results of our kinetic experiments. Under the applied conditions, the activity of CoMo/C (18 mol/(mol of Mo h); 60 mol/(mol of Co h)) on a per mole total metal basis (13.8 mol/(mol of metal h)) is even higher than that of Rh/C.

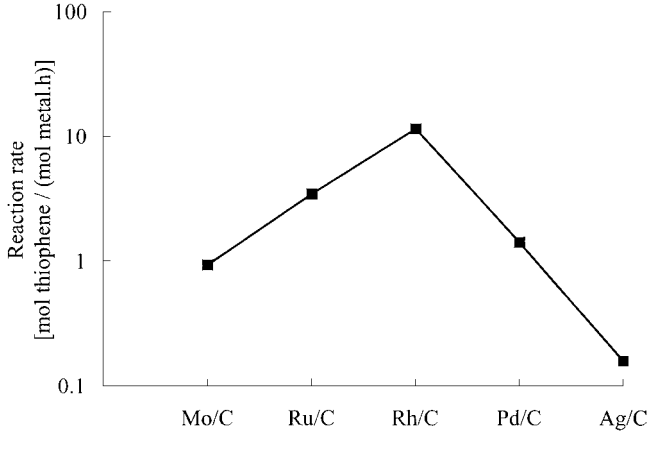

FIG. 1. Thiophene HDS activity for the different carbon-supported TMSs at standard conditions (3.33 kPa thiophene, 1 kPa H_2S, and 573 K).

TABLE 2

Reaction Orders of Thiophene (n_T), H_2S (n_S), H_2 (n_H),[a] and Hydrothiophenes Selectivity (S_{HT}) at Different Conditions

	$T = 573$ K					$T = 623$ K			
Catalyst	n_T[b]	n_T[c]	n_S	n_H[b]	n_H[c]	n_T[c]	n_S	n_H[c]	S_{HT} (%)[d]
Mo/C	0.40	0.50	−0.32	0.54	0.57	0.65	−0.34	0.74	13
Ru/C	0.28	0.39	−0.25	0.56	0.53	0.57	−0.27	0.93	4
Rh/C	0.21	0.31	−0.83	0.71	0.93	0.53	−0.59	1.03	0.5
Pd/C	0.50	0.65	−1.04	0.77	0.99	0.77	−0.97	1.42	19
CoMo/C	0.10	0.12	−0.46	0.61	0.78	0.28	−0.30	0.92	2

[a] 95% confidence interval for n_T, ±0.05; n_S, ±0.07; n_H, ±0.02.
[b] Inlet H_2S partial pressure: 0 kPa.
[c] Inlet H_2S partial pressure: 1 kPa.
[d] Conditions: 3.33 kPa thiophene; 1 kPa H_2S.

Reaction Orders of Thiophene, H_2S, and H_2

In Table 2 the various reaction orders of thiophene, H_2S, and H_2 determined at two different temperatures are listed. While the thiophene reaction orders for Rh/C agree rather well with earlier work (25), the higher reaction orders found for Mo/C (compare these to $n_T = 0.39$ at 573 K and $n_T = 0.50$ at 623 K in Ref. (25)) most probably stem from a difference in the preparation method. In the previous case, an aqueous solution of AHM was used instead of an ammoniacal solution of AHM. Ledoux *et al.* (8) already found that the apparent activation energy for carbon-supported Mo sulfide depends on the metal loading. This indicates that the particle size influences the intrinsic kinetics of thiophene HDS. Furthermore, the use of a mass flow controller for adding H_2S to the reactor feed leads to more precise values for the H_2S inlet pressure as opposed to those of the previous study (25). The very low thiophene reaction orders for CoMo/C are close to the values previously reported (25).

Within the series of 4*d* TMS, the lowest thiophene reaction order is found for the most active catalyst (Rh/C), while the thiophene reaction order for CoMo/C is lowest. As expected, H_2S inhibits the thiophene HDS reaction leading to negative H_2S reaction orders. Strikingly, the H_2S reaction orders vary only a little with temperature for Mo/C, Ru/C, and Pd/C and to a larger extent for CoMo/C and Rh/C. Moreover, the H_2S reaction orders tend to decrease, going from the left-hand side to the right-hand side in the periodic table. Both n_T and n_H at 573 K have been determined (i) in the absence of H_2S and (ii) in the presence of 1×10^3 Pa H_2S. The thiophene reaction orders are higher when H_2S is added to the feed, which can be tentatively explained by competitive adsorption between H_2S and thiophene, leading to a lower thiophene surface coverage. While the effect on n_H for Mo/C and Ru/C is negligible, the change in H_2S

TABLE 3

Activities and Kinetic Parameters for Sulfided and Reduced Pd/C

Catalyst	Reaction rate (mol/(mol h))	n_T[a]	n_H[b]
	$T = 573$ K, H_2S partial pressure: 0 kPa		
Pd/C (sulfided)	13	0.50	0.77
Pd/C (reduced)	16	0.46	0.80
	$T = 573$ K, H_2S partial pressure: 1 kPa		
Pd/C (sulfided)	1.4	0.65	0.99
Pd/C (reduced)	1.7	0.69	0.96

[a] 95% confidence interval: ±0.05.
[b] 95% confidence interval: ±0.02.

TABLE 4

Apparent Activation Energies[a] and Pre-exponential Factors

	Temp. traject: 553–593 K		Temp. traject: 603–643 K	
Catalyst	E_{act} (kJ/mol)	ν_{pre} (573 K)[b]	E_{act} (kJ/mol)	ν_{pre} (623 K)[b]
Mo/C	66	3×10^2	60	5×10^0
Ru/C	75	2×10^4	69	3×10^2
Rh/C	118	3×10^8	82	8×10^2
Pd/C	58	5×10^1	54	2×10^{-2}
CoMo/C	108	8×10^7	72	8×10^{-1}

[a] 95% confidence interval: ±5 kJ/mol.
[b] Unit pre-exponential factors in mol of thiophene/(mol of metal h).

partial pressure influences the H_2 reaction order for Rh/C and Pd/C, suggesting competitive adsorption of H_2S and H_2. The H_2 reaction order tends to increase both going from left to right in the periodic table and with temperature. The selectivity to hydrothiophene product molecules that mainly consist of tetrahydrothiophene is also included in Table 2. It appears that the catalysts with the lowest desulfurization activity show the highest selectivity for these hydrogenation products. As outlined in a previous paper (25), the equilibrium concentration of hydrogenated products decreases with an increasing desulfurization rate. The trend in selectivity complies with the trend in HDS activity.

To study the possible occurrence of different Pd sulfide phases in Pd/C, kinetic parameters (n_T and n_H) were determined at 573 K for sulfided and reduced Pd/C (Table 3). Reduced Pd/C was obtained by exposing the catalyst to a flow of 60 ml/min H_2 while heating at a rate of 6 K/min to 723 K. The temperature was kept at this temperature for 2 h. One set of measurements was performed in the absence of H_2S at the reactor inlet. Typical thiophene conversions were below 5%, leading to an average H_2S partial pressure of 80 Pa over the catalyst bed. This partial pressure is much lower than that in the second set of measurements, which was performed in the presence of 1 kPa H_2S. The kinetic parameters for these catalysts are similar, indicating that it is the applied H_2S/H_2 ratio rather than the pretreatment procedure (sulfidation or reduction) that determines the composition of the active phase.

Activation Energy and Pre-exponential Factor

In Table 4, apparent activation energies and pre-exponential factors are presented. The apparent activation energy was determined in two temperature trajectories, i.e. 533–593 and 603–643 K. One notes that for Mo/C, Ru/C, and Pd/C the apparent activation energy only decreases a little with temperature, while the effect for Rh/C and CoMo/C is more pronounced. Since the reaction orders of thiophene, H_2S, and H_2 are known for the present set of catalysts, the calculated pre-exponential factors are independent of the partial pressure of these components. This explains the different values in the present and previous work (25).

H_2–D_2 Equilibration Activities

In Table 5, the H_2–D_2 equilibration activities (r_{HD}) for the various monometallic TMSs at a temperature of 423 K are collected. The activities were measured at three different initial pressure combinations of H_2, D_2, and H_2S: (i) $P_{H_2} = 3.25$ kPa, $P_{D_2} = 6.5$ kPa, $P_{H_2S} = 0$ kPa (molar ratio $H_2 : D_2 : HD = 1 : 2 : 0$); (ii) $P_{H_2} = 6.5$ kPa, $P_{D_2} = 6.5$ kPa, $P_{H_2S} = 0$ kPa (2 : 2 : 0); and (iii) $P_{H_2} = 3.25$ kPa, $P_{D_2} = 3.25$ kPa, $P_{H_2S} = 3.25$ kPa (1 : 1 : 1). In the standard situation (ii), Ru/C and Rh/C have similar activities. The activity of Mo/C is somewhat lower and Pd/C shows a very low activity. The resulting activity variations are much smaller than those observed for thiophene HDS. This result implies that the rate-limiting step in thiophene HDS is not the same as the rate-limiting step in H_2–D_2 equilibration, as was concluded previously (24, 27). The activities in experiment (i) were lower than those in experiment (ii) due to the lower H_2 partial pressure. As was outlined by Hensen *et al.* (24), these data indicate that H_2 adsorption is rate limiting for Mo/C. For Ru/C and Rh/C, a surface reaction appears to be the rate-limiting step. This may be the surface migration of H(D) species (24, 27). Alternatively, the desorption of hydrogen species can be proposed as the rate-limiting step for

TABLE 5

H_2–D_2 Equilibration Activities (r_{HD}) at 423 K

	r_{HD} (mol of HD/(mol of metal h)) molar ratio $H_2 : D_2 : H_2S$		
Catalyst	1 : 2 : 0	2 : 2 : 0	1 : 2 : 1
Mo/C	1.4	2.8	2.0
Ru/C	2.0	3.5	1.0
Rh/C	2.4	3.6	2.4
Pd/C	n.d.	0.1	0.03

Note. n.d. = not determined.

TABLE 6

r_{HD} as a Function of the Pretreatment H_2S/H_2 Ratio at 573 K

Catalyst	r_{HD} (mol of HD/(mol of metal h))		
	$H_2S/H_2 = 0.1$	$H_2S/H_2 = 0.01$	$H_2S/H_2 = 0.001$
Mo/C	4.8	5	5.2
Ru/C	5.2	5.5	5.8
Rh/C	5.3	5.8	6.3
Pd/C	2.5	3.6	4.8

Rh/C because the rate is proportional to the H surface coverage (after all, the rate is proportional to the square root of the H_2 partial pressure). Rh/C thus shows qualitatively the same behavior as CoMo/C (24).

The addition of H_2S (compare situation (iii) with (i)) leads to an increase of the equilibration activity for Mo/C. Since H_2 adsorption seems to be rate limiting for this catalyst, the increase in H surface coverage as a result of the dissociative adsorption of H_2S provides an explanation for the promotional effect of H_2S. While the effect for Ru/C and Pd/C is negative, to be attributed to competitive adsorption between H_2S and H_2, there is no apparent effect of the addition of H_2S upon comparison of experiments (i) and (iii) for Rh/C. This most probably relates to a stronger activation of H_2S by Rh/C, resulting in an easier exchange of H atoms originating from H_2S.

The H_2–D_2 equilibration activities for the different TMSs at 573 K are listed in Table 6 as a function of the H_2S/H_2 ratio during the final sulfiding step. Clearly, a lower H_2S/H_2 ratio leads to a higher r_{HD} for all catalysts. This can be tentatively explained by the differences in sulfur coordination as a result of the different applied H_2S/H_2 ratios. For the 4*d* TMS, the effect is more pronounced, going from Mo/C to Pd/C. An additional H_2–D_2 equilibration experiment was carried out in which Pd/C was reduced according to the aforementioned procedure. The reaction temperature was again 573 K. Although the initial activity, i.e., $r_{HD} = 5.9$ mol of HD/(mol of Pd h), is higher than that of Pd/C sulfided at $H_2S/H_2 = 0.001$, the amount of H_2, HD, and D_2 species in the gas phase quickly decreased. This points to the presence of metallic Pd particles, which are known to form Pd–hydride (28), and Pd–deuteride in our case.

DISCUSSION

Within the series of 4*d* TMS, the most active catalyst, i.e., Rh/C, exhibits the lowest thiophene reaction order. A low thiophene reaction order is indicative of a strong thiophene–TMS interaction. This was derived from a kinetic model representing a simplified Langmuir–Hinshelwood approach, as presented in a previous paper (25). The most important finding in that study was that the most active catalyst (CoMo/C) has the lowest thiophene reaction order (0.1 at 573 K) among a series of carbon-supported Mo, Co, CoMo, and Rh sulfide catalysts. This strong interaction leads to activation of the C–S bond in thiophene and a higher HDS reaction rate. The surface of CoMo/C is taken to be totally covered by thiophene at the applied conditions. This proposal was refined in the sense that a thiophene reaction order close to zero may also point to the formation of a strongly adsorbed intermediate (e.g., a dihydrothiophene or tetrahydrothiophene) or the removal of a strongly adsorbed dissociated complex (21). Within the present series, we infer that the highest activity is found for the catalyst with the highest thiophene–TMS interaction energy. This strong interaction for Rh/C results in relatively large changes in surface coverage as a function of temperature. This is validated by the large change in thiophene reaction order for this catalyst compared to that of the less active ones, as can be found in Table 2. As noted before, the effect of the inlet H_2S partial pressure on the thiophene reaction orders is due to competitive adsorption between thiophene and H_2S. This effect is smallest for CoMo/C, which corroborates with a nearly totally covered surface as suggested from the low thiophene reaction orders.

The trends in thiophene reaction orders will be discussed in the light of Sabatier's principle (6, 29, 30) and the "bond energy model" by Nørskov *et al.* (19). In the case Sabatier's principle applies, a low thiophene–TMS interaction energy results in difficult formation of the reaction intermediate, while a strong interaction leads to an unreactive intermediate; i.e., hydrogenative sulfur removal becomes the rate-limiting step. As outlined by Hensen *et al.* (21), this implies a positive thiophene reaction order for a heat of adsorption well below the optimum, and a zero (negative in the case of dissociative adsorption) reaction order for too strong interaction between thiophene and the TMS surface. Both from the experimental heat of formation of the bulk TMS (6) as well as from calculated bulk metal–sulfur bond strengths (29, 30), it follows that MoS_2 has the highest metal–sulfur bond strength within our set of catalysts. Going from MoS_2 to PdS, this metal–sulfur bond strength decreases. Hence, the present trend in thiophene reaction orders is conflicting with such an interpretation. According to the proposal of Nørskov, Clausen, and Topsøe (19), the highest activity is found for the TMS with the lowest metal–sulfur bond energy due to the largest number of coordinatively unsaturated sites. Unfortunately, there is currently no accurate method for determining the number of coordinatively unsaturated sites. The kinetic implication of this proposal is that the highest thiophene reaction order is found for the most active catalyst as long as there is no change in the rate-limiting step as a function of catalyst composition. However, the present kinetic data show that the interaction is strongest for the most active TMS. Hence, it is tentatively concluded that the trend in intrinsic chemistry of the

various TMSs is counter to the proposal advocated by Nørskov *et al.* (19).

These apparent conflicts require a closer look at the kinetic data at issue. The H_2S orders are highest for Mo/C and Ru/C and decrease going to the right-hand side of the periodic table. However, from bulk metal–sulfur bond strength considerations, one would expect the most negative H_2S reaction order for Mo/C. For Mo/C, Ru/C, and Pd/C, the H_2S reaction orders depend little on temperature, which points to a low metal–sulfur bond energy. The relatively large change in H_2S reaction order for Rh/C with temperature agrees with the proposal of the highest metal–sulfur bond energy for this catalyst.

The dependence of the H_2 reaction order on the H_2S partial pressure for Rh/C and Pd/C (Table 2) can be tentatively interpreted in terms of competitive adsorption of H_2S and H_2. The fact that this H_2S dependency is absent for the other two catalysts can be ascribed to the presence of different H_2S and H_2 adsorption sites. On the other hand, one notes that the H_2S reaction orders for Mo/C and Ru/C are close to zero and that they hardly vary with temperature: this can be interpreted in terms of a lower H_2S surface coverage, leading to a higher H_2 surface coverage and consequently lower H_2 reaction orders. In short, the increase in H_2 reaction order going from left to right in the periodic table is consistent with an increasing H_2S coverage.

Altogether, these findings are counter to the commonly held notion of Sabatier behavior for these catalysts; that is to say, the present kinetic data necessitate a new interpretation of the role of the metal–sulfur bond energy at the TMS surface. The conventional application of Sabatier's principle to TMS is to correlate the interaction between TMS and the reaction intermediate with the bulk metal–sulfur bond energy, that is, considered independent from sulfur coordination number. This energy is derived from the bulk metal–sulfur bond strength of the thermodynamically most stable compounds (6, 29, 30). The "bond energy model" also implies that the metal–sulfur bond energy at the TMS surface directly correlates with the bulk metal–sulfur bond energy. However, the relevant metal–sulfur bond energy is the one at the TMS surface and strongly depends on the sulfur coordination of the TM atoms at this surface under reaction conditions. The sulfur coordination may be very different from the bulk situation. Going from left to right in the periodic table the stability of TMS decreases due to a decreasing metal–sulfur bond strength. The H_2S/H_2 equilibrium ratios for the reduction of the bulk TMS 600 K calculated from thermodynamic data (31, 32) are given in Table 7. It follows that the stability of the TMS decreases going from MoS_2 to PdS. It is evident that, under the applied reaction conditions, i.e., $0.001 < H_2S/H_2 < 0.02$, Pd and Rh may not be present as completely sulfided phases, whereas Mo/C and Ru/C form stable TMS phases. Additionally, the degree of coordinative unsaturation may play an important role. This was already outlined by Pecoraro and Chianelli (6) for Ru, Rh, and Pd sulfide, and they actually estimated from XRD measurements that Ru sulfide had lost some sulfur under their reaction conditions.

TABLE 7

H_2S/H_2 Equilibrium Ratios for the Reduction of Bulk TMS at 600 K

Equilibrium	H_2S/H_2 equilibrium ratio
$Mo + 2H_2S \leftrightarrow MoS_2 + 2H_2$	4×10^{-7}
$Ru + 2H_2S \leftrightarrow RuS_2 + 2H_2$	9×10^{-5}
$2RhS_{0.9} + 1.2H_2S \leftrightarrow Rh_2S_3 + 1.2H_2$	1×10^{-2}
$Rh + 0.9H_2S \leftrightarrow RhS_{0.9} + 0.9\ H_2$	9×10^{-5}
$Pd + H_2S \leftrightarrow PdS + H_2$	3×10^{-1}

Note. The crystal structure of $RhS_{0.9}$ is most probably $Rh_{17}S_{15}$ (8).

The sulfur addition energy, i.e., the energy associated with the addition of a sulfur atom to an incompletely sulfided transition metal cluster, tends to decrease with the number of added sulfur atoms, as expected from the bond order conservation (BOC) principle (33, 34). This was nicely demonstrated for sulfur addition to Ni_3S_x clusters in a theoretical study by Neurock and Van Santen (34). TMSs at the left-hand side of the periodic table tend to form stable sulfide phases. Hence, the interaction energy between the TMS and H_2S (or thiophene), which can be assumed to be proportional to the sulfur addition energy in a first analysis, is low for these stable sulfides. When the stability of the TMS decreases, this leads to a higher degree of coordinative unsaturation. Although the bulk metal–sulfur bond energy of a TMS at the right-hand side of the periodic table is lower than that of one at the left-hand side, the sulfur addition energy may be higher due to the higher degree of sulfur deficiency at the TMS surface. Further reduction of the bulk metal–sulfur bond energy may also lead to the formation of sulfide phases with a lower sulfur coordination number. At the extreme right of the periodic table, the sulfur addition energy will also decrease due to weak metal–sulfur interaction energies.

Conceptually, this can be understood in terms of the metal–sulfur bond energy at the surface being highly dependent on the sulfur coordination of the surface metal atoms. The differential increase in metal–sulfur bond strength as a function of degree of sulfur removal is higher for more stable sulfides. In Fig. 2, this concept is visualized by plotting the sulfur addition energy as a function of the degree of sulfur removal. The coordinatively saturated phases (MoS_2, RuS_2, Rh_2S_3, and PdS) are located at the right-hand side. The sulfur addition energy of the respective sulfides is taken to be proportional to the bulk metal–sulfur bond strengths. The curves in Fig. 2 schematically represent the resulting general trend of sulfur addition energy of the various TMSs as a function of sulfur coordination. The sulfur coordination of the stable phases are chosen arbitrarily. The inset shows

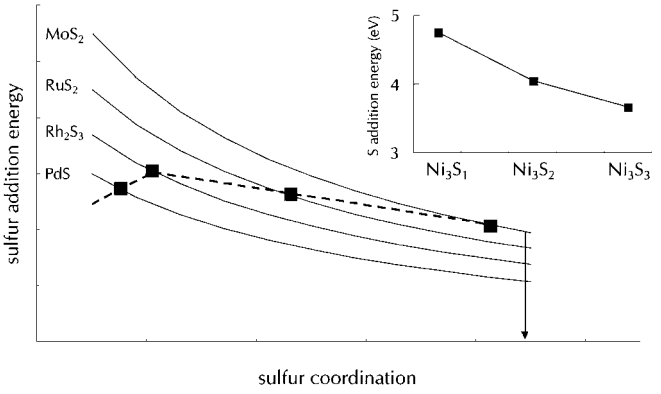

FIG. 2. Sulfur addition energy as a function of sulfur coordination. The dashed line represents a *volcano*-type plot of the sulfur addition energy of the various TMSs. The inset shows the sulfur addition energy for Ni_3S_x clusters calculated from density function theory (35).

the sulfur addition energy for Ni_3S_x clusters calculated using "density functional theory" (35).

The sulfur coordination at the TMS surface is lower than that in the bulk and this leads to an increase of the sulfur addition energy with decreasing sulfur coordination. The increase is largest for the TMS with the highest bulk metal–sulfur bond energy. The pivotal point is the lower sulfur coordination of the surface metal atoms of the TMSs at the right-hand side of the periodic table compared to the ones at the left-hand side. This is due to the weaker metal–sulfur bond energies at the right of the periodic table. The dashed line in Fig. 2 tallies with a situation in which these sulfur addition energy changes will result in a *volcano*-type behavior of the HDS reaction rate as a function of the periodic position. This represents our proposed conjecture on the relation between HDS activity and sulfur addition energy. A similar relation, but then with the metal–oxygen bond energy, has been presented by Sachtler and co-workers (36) for the partial oxidation of benzaldehyde over transition metal oxides. It was found that the selectivity is at its maximum for the catalyst with the highest differential increase of metal–oxide bond strength as a function of degree of reduction.

When this sulfur addition energy concept is applied to our set of 4*d* TMS, the starting point is that MoS_2 forms the most stable sulfide phase with the highest bulk metal–sulfur bond energy. The interaction with H_2S or organic sulfides is weak due to the low energy gained upon the addition of an extra sulfur atom. This results in relatively high thiophene and less negative H_2S reactions orders. The decrease in bulk metal–sulfur bond energy going to RuS_2 and Rh_2S_3 leads to a higher degree of coordinative unsaturation. The sulfur addition energy at the TMS surface of Rh_2S_3 is higher than that of MoS_2, although these energies show an opposite trend in the bulk (6, 29). This is reflected by lower thiophene and H_2S reaction orders going to the right-hand side of the periodic table. The metal–sulfur bond energy for Pd/C has become so low that in spite of the high sulfur deficiency the interaction energy with thiophene is lower than that for Rh/C. This forms the explanation for the higher thiophene reaction order of Pd/C and the lower HDS activity. This only leaves the H_2S reaction order in need of an explanation: although it does not vary significantly with temperature, the reaction order is close to −1, suggesting a strong interaction between the TMS and H_2S. Alternatively, this value may reflect the fact that different Pd sulfide phases are present at the various applied H_2S partial pressures. The HDS activities of these phases may be very distinct. A close inspection of the phase diagram of the Pd–S system (37) reveals that Pd sulfide can be present in different sulfide phases in the range of the H_2S/H_2 ratios applied in this study (Fig. 3): Pd metal (at a H_2S/H_2 ratio below 0.008), Pd_4S (at H_2S/H_2 ratios between 0.008 and 0.025), and PdS at higher ratios. The Pd ions in Pd_4S are coordinated only by two sulfide ions, but also by ten nearby Pd ions, at a distance ranging from 277 to 312 pm; the Pd–Pd separation in the Pd metal is 275 pm (38). The applied H_2S partial pressures are too low for the formation of PdS_2. In addition to Pd_4S, also phases such as Pd_3S and $Pd_{16}S_7$ may be formed for which no thermodynamic data are available. In conclusion, the strongly poisoning effect of H_2S on Pd/C can be substantiated by the notion that different sulfide phases and most probably a metallic phase at the lowest H_2S partial pressures with very different intrinsic activities are present. The large change in H_2 reaction order for Pd/C can now be rationalized by the presence of different Pd–S phases present as a function of the H_2S partial pressure. As can be seen from Table 2, Rh/C also shows such a large change in H_2 reaction order, while this parameter is nearly constant for Mo/C and Ru/C. Alternative to the suggestion of different H_2S and H_2 adsorption sites for these catalysts, this may indicate that also different Rh sulfide phases are present as a function of H_2S partial pressure (e.g., the transition Rh_2S_3 to $RhS_{0.9}$ as suggested in Table 7), whereas Mo/C and Ru/C retain the same sulfide phase under the applied conditions.

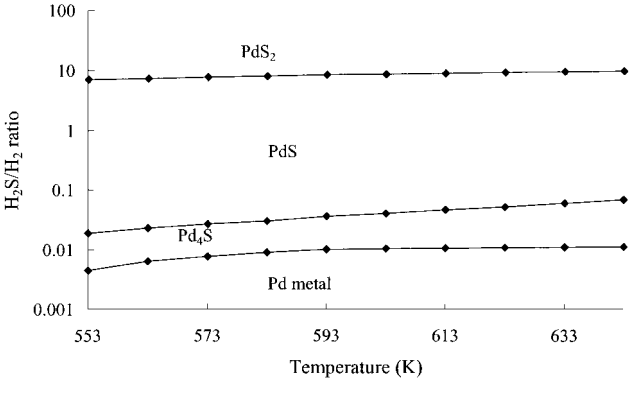

FIG. 3. Phase diagram of the Pd–S system in the relevant regime of our reaction conditions.

The activities as well as thiophene and H_2 reaction orders of sulfided Pd/C and reduced Pd/C were determined both in the presence of H_2S (1 kPa) and in the absence of H_2S (Table 3). The lower reaction orders at 0 kPa H_2S inlet pressure compared to those at 1 kPa H_2S inlet pressure are indicative for the stronger adsorption of thiophene and H_2 on the metallic Pd phase. The average H_2S/H_2 ratio over the catalyst bed resulting from thiophene decomposition is approximately 8×10^{-4}, resulting in the presence of metallic Pd particles according to thermodynamics (Fig. 3). It follows that the applied H_2S/H_2 ratio under reaction conditions is a more important factor on the sulfur coordination in Pd sulfide than the applied H_2S/H_2 ratio during sulfidation. Also, the H_2–D_2 equilibration experiments at 573 K using different H_2S/H_2 ratios in the final sulfiding step are instructive in this. The activity changes between the different experiments become larger going from the left-hand side to the right-hand side in the periodic table. In line with the expected large variations in sulfur coordination for Pd/C, the activity differences for differently pretreated Pd/C are largest. Our data also suggest that after sulfidation at a H_2S/H_2 ratio of 0.001 no metallic Pd is formed, which is consistent with the thermodynamic data. When Pd/C is reduced, the initial equilibration activity is highest, although in this case Pd–hydride and Pd–deuteride form and the gas-phase concentrations of hydrogen species quickly decrease. In conclusion, the H_2–D_2 equilibration activity results at 573 K are consistent with our picture of a decreasing sulfur coordination going to the less stable TMS.

The apparent activation energies based on the reaction rate measurements in two temperature trajectories, i.e., 553–593 and 603–643 K, are given in Table 4. The pre-exponential factors have been calculated at 573 and 623 K using the reaction orders in thiophene, H_2S, and H_2. In accordance with previous results (25), Rh/C shows a clear infliction point in an Arrhenius plot. It is suggested that this originates from a phase transition between Rh_2S_3 at temperatures below 583 K and $Rh_{17}S_{15}$ at higher temperatures. Previously, a change in the rate-limiting step was put forward as an explanation for the different apparent activation energies of these two phases (25). Alternatively, the present analysis provides a more subtle explanation. The sulfur coordination in the sulfur-deficient Rh sulfide phase ($Rh_{17}S_{15}$) is lower, leading to a higher bulk metal–sulfur bond energy. In addition to the effect of thiophene surface coverage, these changes in sulfur coordination may also influence the apparent activation energy. This can be interpreted as an alternative explanation for the lower apparent activation energy of the high-temperature phase.

While this transition in apparent activation energy is clear for Rh/C, it appears that the other catalysts show a slowly decreasing apparent activation energy with increasing temperature. In Fig. 4, an Arrhenius plot for Mo/C clearly shows this effect. At high temperatures ($T > 703$ K), the activity of Mo/C drops due to irreversible deactivation most probably caused by sintering of the active phase. Irreversible sulfur removal is an alternative explanation for this loss of activity. While the apparent activation energy for Mo/C amounts to 66 kJ/mol at 573 K, the activation energy drops to 50 kJ/mol at 673 K. The values for the apparent activation energies in two different temperature trajectories show this behavior (Table 4). This decrease in apparent activation energy with increasing temperature can be understood in terms of surface coverages of reactants and products. When a simplified Langmuir–Hinshelwood-type mechanism is assumed for the thiophene HDS reaction at the TMS surface, we find for the reaction rate

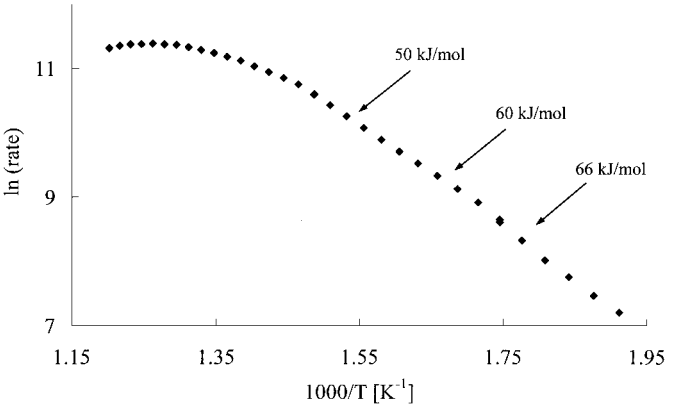

FIG. 4. Arrhenius plot for Mo/C (indicated: apparent activation energies).

$$r = k \cdot \Theta_T, \qquad [2]$$

$$r = k \cdot \frac{K_T \cdot P_T}{1 + K_T \cdot P_T + K_S \cdot P_S}, \qquad [3]$$

with $\Theta_T(\Theta_S)$ = the surface coverage of thiophene (H_2S), $K_T(K_S)$ = the adsorption constant of thiophene (H_2S), and $P_T(P_S)$ = the partial pressure of thiophene (H_2S).

When the reaction rate constant k has an Arrhenius-type behavior and can be considered independent of surface coverage, one can derive the exact result

$$E_{act}^{app} = -R_g \frac{\partial \ln r}{\partial T^{-1}} = E_{act}^{rls} + (1 - \Theta_T) \cdot \Delta H_{ads}^{T} - \Theta_S \cdot \Delta H_{ads}^{S}, \qquad [4]$$

with E_{act}^{app} = the apparent activation energy, E_{act}^{rls} = the true activation energy of the rate-limiting step, and ΔH_{ads}^{T} (ΔH_{ads}^{S}) = the heat of adsorption of thiophene (H_2S). This expression for the apparent activation energy is an extension of the one described by Hensen *et al.* (21, 25) and by Van Santen and Niemantsverdriet (39). The surface coverage of both thiophene and H_2S decrease with increasing temperature, resulting in a lower apparent activation energy (Eq. [4]). This effect is more pronounced for catalysts

with a high heat of adsorption of sulfur-containing molecules. The changes in apparent activation energy are in line with this interpretation. Moreover, the largest decrease in apparent activation energy for Rh/C and CoMo/C fully complies with the proposal of the highest sulfur addition energy for these catalysts.

The high pre-exponential factor for the most active catalysts can be explained by a strong interaction of the TMS with the adsorbed complex. The increase in entropy during the rate-limiting step—most probably C–S bond breaking (25)—is highest. This is in line with our interpretation of the trends in the measured reaction orders and apparent activation energies. Since no accurate method is available for measuring the active site density in TMS, the number of active sites is also included in this pre-exponential factor. However, from the very large differences in the pre-exponential factor between the various TMSs, we conclude that variations in active site densities cannot be the explanation for the periodic trends in thiophene HDS. A high interaction energy between the TMS and reactant plays a crucial role in explaining the high HDS activity of Rh/C and CoMo/C. In the case of the 4*d* TMS series, it is inferred that this interaction energy depends on the sulfur coordination of the TMS surface. The sulfur coordination decreases going from left to right in the periodic table, resulting in large activity variations. The high activity of CoMo/C appears also to be related to such a strong interaction between the TMS and thiophene. It is instructive to relate the present conjecture relating metal–sulfur bond strength at the TMS surface and thiophene HDS activity to previous ones that refer to bulk metal–sulfur bond strengths. The direct correlation between bulk metal–sulfur bond energies and intrinsic chemistry at the TMS surface may be more complicated. For instance, the proposed weakening of the Co–S–Mo lattice bond strength in "Co–Mo–S" (40) can lead to a higher electron density in the coordination sphere of Co (BOC principle), resulting in a stronger interaction with the reactant. It appears paramount to calculate the metal–sulfur bond energies at the TMS surface and verify them experimentally at *in situ* conditions.

CONCLUSIONS

It has been found that the thiophene HDS kinetics for a set of 4*d* TMS cannot be accounted for by the prevailing theories that relate HDS activities to bulk metal–sulfur bond strengths. From the present study, it follows that high HDS activities are found for those catalysts having a low thiophene reaction order and a high apparent activation energy. A high HDS activity is linked to a strong thiophene–TMS interaction. This is fortified by large changes in thiophene and H_2S surface coverage and apparent activation energies as a function of temperature. It is suggested that due to the decreasing bulk metal–sulfur bond strength going from the left to the right in the periodic table, the metal–sulfur bond strength at the TMS surface (sulfur addition energy), which is relevant to catalysis, shows *volcano*-type behavior. This sulfur addition energy is low for the most stable sulfide (MoS_2) due to complete sulfur coordination of Mo. The decrease in bulk metal–sulfur bond strength results in more coordinative unsaturation for the sulfides to the right-hand side of the periodic table. Hence, the sulfur coordination of the TMS surface is decreased, leading to a higher sulfur addition energy and concomitant stronger activation of thiophene. It is proposed that the bulk Pd–S bond strength is so low that the sulfur addition energy decreases at the right-hand side of the periodic table. This low bulk metal–sulfur bond strength results in the formation of Pd sulfide phases with a lower sulfur coordination and possibly Pd metal, depending on the applied H_2S/H_2 ratio. H_2–D_2 equilibration experiments show that the equilibration activity increases with a decreasing H_2S/H_2 ratio during sulfidation, to be explained by a higher degree of coordinative unsaturation. This effect becomes larger for the least stable sulfides, in agreement with our proposal. The kinetics for CoMo/C show that a high sulfur addition energy is important in explaining the high HDS activity of the promoted catalyst.

ACKNOWLEDGMENTS

These investigations have been supported by the Netherlands Foundation for Chemical Research (SON) with financial aid from the Netherlands Technology Foundation (STW). The research has been performed under the auspices of NIOK, the Netherlands Institute for Catalysis Research, Lab Report TUE-99-5-09.

REFERENCES

1. Chianelli, R. R., *Catal. Rev.-Sci. Eng.* **26**, 361 (1984).
2. Prins, R., De Beer, V. H. J., and Somorjai, G. A., *Catal. Rev.–Sci. Eng.* **31**, 1 (1989).
3. Wiegand, B. C., and Friend, C. M., *Chem. Rev.* **92**, 491 (1992).
4. Topsøe, H., Clausen, B. S., and Massoth, F. E., "Hydrotreating Catalysis." Springer, Berlin, 1996.
5. Eijsbouts, S., *Appl. Catal. A* **158**, 53 (1997).
6. Pecoraro, T. A., and Chianelli, R. R., *J. Catal.* **67**, 430 (1981).
7. Vissers, J. P. R., Groot, C. K., Van Oers, E. M., De Beer, V. H. J., and Prins, R., *Bull. Soc. Chim. Belg.* **93**, 813 (1984).
8. Ledoux, M. J., Michaux, O., Agostini, G., and Panissod, P., *J. Catal.* **102**, 275 (1986).
9. Harris, S., *Chem. Phys.* **67**, 229 (1982).
10. Harris, S., and Chianelli, R. R., *Chem. Phys. Lett.* **101**, 603 (1983).
11. Harris, S., and Chianelli, R. R., *J. Catal.* **86**, 400 (1984).
12. Harris, S., and Chianelli, R. R., *J. Catal.* **98**, 17 (1986).
13. Smit, T. S., and Johnson, K. H., *Chem. Phys. Lett.* **212**, 525 (1993).
14. Smit, T. S., and Johnson, K. H., *J. Mol. Catal.* **91**, 207 (1994).
15. Smit, T. S., and Johnson, K. H., *Catal. Lett.* **28**, 361 (1994).
16. Rong, C., and Qin, X., *J. Mol. Catal.* **64**, 321 (1991).
17. Rong, C., Qin, X., and Jinglong, H., *J. Mol. Catal.* **75**, 253 (1992).
18. Zonnevylle, M. C., Hoffman, R., and Harris, S., *Surf. Sci.* **199**, 320 (1988).
19. Nørskov, J. K., Clausen, B. S., and Topsøe, H., *Catal. Lett.* **13**, 1 (1992).

20. Topsøe, H., Clausen, B. S., Topsøe, N.-Y., Hyldtoft, J., and Nørskov, J. K., *Symp. Prepr. Am. Chem. Soc. Div. Petr. Chem.* **38**, 638 (1993).
21. Hensen, E. J. M., De Beer, V. H. J., and Van Santen, R. A., *in* "Transition Metal Sulphides: Chemistry and Catalysis" (Th. Weber, R. Prins, and R. A. Van Santen, Eds.), p. 169. Kluwer, Dordrecht, 1998.
22. Vissers, J. P. R., De Beer, V. H. J., and Prins, R., *J. Chem. Soc. Faraday Trans. 1* **83**, 2145 (1987).
23. Van Veen, J. A. R., Gerkema, E., Van der Kraan, A. M., and Knoester, A., *J. Chem. Soc. Chem. Commun.* 1684 (1987).
24. Hensen, E. J. M., Lardinois, G. M. H. J., De Beer, V. H. J., Van Veen, J. A. R., and Van Santen, R. A., *J. Catal.* **187**, 95 (1999).
25. Hensen, E. J. M., Vissenberg, M. J., De Beer, V. H. J., Van Veen, J. A. R., and Van Santen, R. A., *J. Catal.* **163**, 429 (1996).
26. Weisser, O., and Landa, S., "Sulfide Catalysts, Their Properties and Applications." Pergamon, New York, 1973.
27. Thomas, C., Vivier, L., Lemberton, J. L., Kasztelan, S., and Pérot, G., *J. Catal.* **167**, 1 (1997).
28. Palladium (System Number 65), "Gmelin Handbook of Inorganic Chemistry." Springer, Berlin, 1941.
29. Raybaud, P., Kresse, G., Hafner, J., and Toulhoat, H., *J. Phys.: Condens. Matter* **9**, 11085 (1997).
30. Raybaud, P., Hafner, J., Kresse, G., and Toulhoat, H., *J. Phys.: Condens. Matter* **9**, 11107 (1997).
31. Mills, K. C., "Thermodynamic Data for Inorganic Sulfides, Selenides and Tellurides." Butterworths, London, 1974.
32. Kubaschewski, O., and Alcock, C. B., "Metallurgical Thermochemistry." Pergamon Press, Oxford, 1979.
33. Shustorovich, E., *Surf. Sci. Rep.* **6**, 1 (1986).
34. Shustorovich, E., *Adv. Catal.* **37**, 101 (1990).
35. Neurock, M., and Van Santen, R. A., *J. Am. Chem. Soc.* **116**, 4427 (1994).
36. Sachtler, W. H. M., Dorgelo, G. J. H., Fahrenfort, J., and Voorhoeve, R. J. H., "Reprints of the Fourth International Congress on Catalysis, Moscow, 1968" (J. W. Hightower, Ed.), p. 604.
37. Van Veen, J. A. R., personal communication.
38. Genin, H. S., and Ibers, J. A., *in* "Transition Metal Sulphides: Chemistry and Catalysis" (Th. Weber, R. Prins, and R. A. Van Santen, Eds.), p. 1. Kluwer, Dordrecht, 1998.
39. Van Santen, R. A., and Niemantsverdriet, J. W., "Chemical Kinetics and Catalysis." Plenum, New York, 1995.
40. Byskov, L. S., Hammer, B., Nørskov, J. K., Clausen, B. S., and Topsøe, H., *Catal. Lett.* **47**, 177 (1997).